ACS Medicinal Chemistry Letters

Letter

pubs.acs.org/acsmedchemlett

Pyrido[4,3-*e*][1,2,4]triazolo[4,3-*a*]pyrazines as Selective, Brain Penetrant Phosphodiesterase 2 (PDE2) Inhibitors

Frederik J. R. Rombouts,*[,†] Gary Tresadern,[‡] Peter Buijnsters,[†] Xavier Langlois,[§] Fulgencio Tovar,[∥] Thomas B. Steinbrecher,[⊥] Greet Vanhoof,[‡] Marijke Somers,[‡] José-Ignacio Andrés,[#] and Andrés A. Trabanco[#]

[†]Neuroscience-Medicinal Chemistry, [‡]Discovery Sciences, [§]Neuroscience-Biology, Janssen Research & Development, Janssen Pharmaceutica N.V., Turnhoutseweg 30, B-2340 Beerse, Belgium

[∥]Villapharma Research S.L., Parque Tecnológico de Fuente Álamo. Ctra. El Estrecho-Lobosillo, Km. 2,5- Av. Azul, 30320 Fuente Álamo de Murcia, Murcia, Spain

[⊥]Schrödinger GmbH, Dynamostrasse 13, D-68165 Mannheim, Germany

[#]Neuroscience-Medicinal Chemistry, Janssen Research & Development, Janssen-Cilag S.A., C/Jarama 75, 45007 Toledo, Spain

Supporting Information

ABSTRACT: A novel series of pyrido[4,3-*e*][1,2,4]triazolo-[4,3-*a*]pyrazines is reported as potent PDE2/PDE10 inhibitors with drug-like properties. Selectivity for PDE2 was obtained by introducing a linear, lipophilic moiety on the meta-position of the phenyl ring pending from the triazole. The SAR and protein flexibility were explored with free energy perturbation calculations. Rat pharmacokinetic data and *in vivo* receptor occupancy data are given for two representative compounds **6** and **12**.

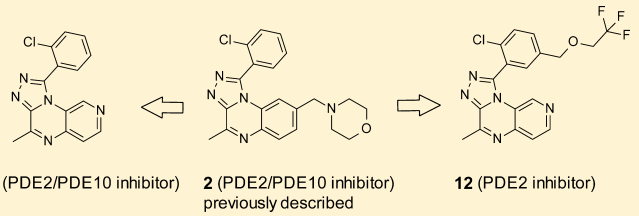

KEYWORDS: *Pyrido[4,3-e][1,2,4]triazolo[4,3-a]pyrazine, PDE2 inhibitor, phosphodiesterase 2 inhibitor, tricycle, selective*

Phosphodiesterases (PDEs) control the degradation of second messengers cAMP and cGMP. Eleven PDE subfamilies with distinct tissue distribution and varying selectivity for cAMP and cGMP have been identified.[1] PDE2 is a dual-substrate enzyme, stimulated by cGMP and degrading both cAMP and cGMP.[2] It is the most abundant PDE subtype in the hippocampus, a brain structure playing an important role in cognitive processes.[3] Cyclic nucleotides are key signaling molecules implicated in the regulation of neuronal plasticity and memory.[4−6] PDE2 inhibition elevates levels of these molecules and could exert procognitive activity and restore hippocampal function, which are altered in disease states such as schizophrenia or Alzheimer's disease.[7] However, the lack of selective and brain penetrant PDE2 inhibitors has hampered validation of this hypothesis in animal models. We have previously reported the optimization of the poorly soluble HTS hit **1** into molecule **2** with combined PDE2/PDE10 activity (Scheme 1). This early lead **2** was valuable for studying CNS effects of PDE2/PDE10 inhibition *in vivo*.[8] More recently, we have described optimization of **2** via structure-based drug design to **3**, a selective and brain penetrant PDE2 inhibitor.[9]

The poor solubility of **1** was addressed in **2** and **3** by substituting the benzo-fused ring of the triazoloquinoxaline core with basic aliphatic amines. While solubility was greatly increased in **2** and **3**, both compounds had poor metabolic stability (Scheme 1). In parallel introduction of pyridyl-like nitrogens in the benzene ring of the quinoxaline moiety was explored, as these could increase solubility while maintaining high ligand efficiency (LE) and good overall physicochemical and ADME properties.

Scheme 1. Optimization of HTS Hit 1 into Lead Compound 3

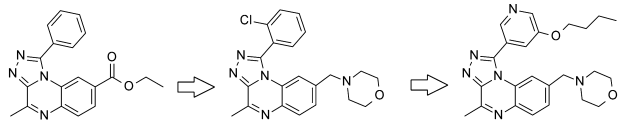

1, HTS hit	**2**, PDE2/PDE10 inhibitor	**3**, PDE2 selective inhibitor
hPDE2 IC_{50} 30 nM	hPDE2 IC_{50} 3 nM	hPDE2 IC_{50} 10 nM
rPDE10 IC_{50} 325 nM	rPDE10 IC_{50} 33 nM	rPDE10 IC_{50} 4823 nM
Formulatability[a] <0.1 mg/mL	Formulatability[b] 6 mg/mL	Formulatability[b] 15 mg/mL
	hLM[c] 98%, rLM[c] 99%	hLM[c] 100%, rLM[c] 100%

[a]Ten percent HPβCD, pH 2. [b]Twenty percent HPβCD, pH 3.6−3.8. [c]Percent metabolized after incubating 1 μM solution 15 min with rLM or hLM at 37 °C.

Prior to synthesis, the four possible isomers bearing a nitrogen atom in the quinoxaline benzene ring (**5**−**8**, Chart 1) were docked into the PDE2 protein using the SP mode of

Received: November 8, 2014
Accepted: January 15, 2015
Published: January 15, 2015

DOI: 10.1021/ml500463t
ACS Med. Chem. Lett. 2015, 6, 282−286

Chart 1. Triazoloquinoxaline 4 and Aza-Analogues 5-8

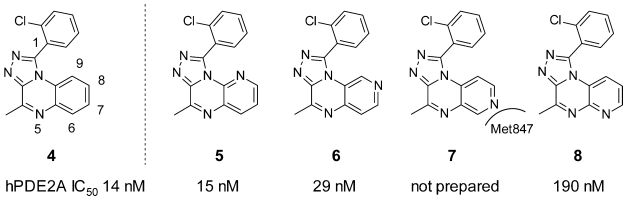

Glide[10] with default protein preparation. A docking protocol with enhanced ligand sampling reproduced the crystal structure binding mode of four different PDE2−inhibitor complexes with good accuracy (see Supporting Information (SI)). Docking helped prioritize **5**, **6**, and **8**, but **7** was not targeted as it presents an unfavorable interaction between the pyridyl nitrogen and Met847 in PDE2. The proximity of this atom to Met847 is revealed by the short 4.3 Å distance between the closest heavy atoms of **9** and Met847 (Figure 1, *vide infra*). For baseline comparison the [1,2,4]triazolo[4,3-*a*]quinoxaline **4** was also synthesized.

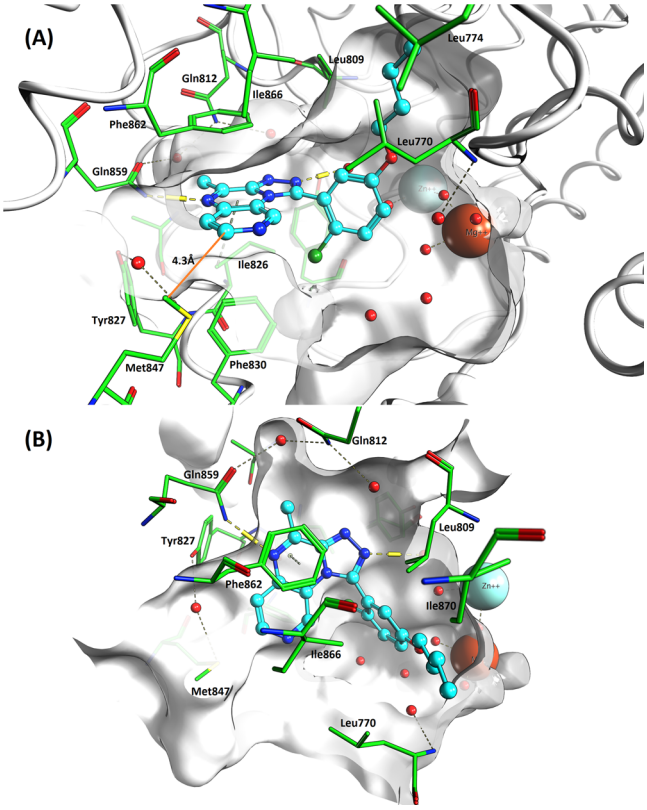

Figure 1. Molecule **9** (cyan color) docked into PDE2A crystal structure solved with **3** (PDB 4D08). Viewed from the entrance to the active site (A) and top down (B). Important amino acids are highlighted in green, and catalytic Zn^{2+} and Mg^{2+} ions are shown, along with active site water molecules (red spheres). Distance between **9** and Met847 highlighted in orange.

Of the three isomers prepared, **5** (IC_{50} = 15 nM) and **6** (IC_{50} = 29 nM) showed comparable inhibitory potency for PDE2 to the carbon analogue **4** (IC_{50} = 14 nM), whereas isomer **8** was 13-fold less potent (IC_{50} = 190 nM).[11] Formulatability of **5** (<0.5 mg/mL with 20% HPβCD at pH 2) was similar to that of the HTS hit **1**; however, the regioisomeric **6** was significantly more soluble (>1 mM in buffer at pH 7.4 and 4 mg/mL with 20% HPβCD at pH 3.9), which can be attributed to the higher solvent exposure and hydrogen bonding capability of the pyridine-like nitrogen in **6**. This is also reflected by their respective experimental pK_a values (**5**, pK_a = 1.0; **6**, pK_a = 2.7). Hence, **6** was selected for further optimization.

The *in vitro* selectivity data of **6** versus other PDE's along with *in vitro* ADME and physicochemical data are summarized in Table 1. Molecule **6** inhibited PDE2 and PDE10,

Table 1. *In Vitro* PDE Selectivity Profile, *in Vitro* ADME, and Physicochemical Properties of 6

PDE selectivity profile		ADME and physicochemical properties	
subtype	IC_{50} (nM)		
hPDE1A	>10000	hLM[a]	7
hPDE2A	**29**	rLM[a]	13
hPDE3B	>10000	kinetic solubility at pH 7.4 (μM)[b]	>1000
hPDE4D	5890	pK_a[c]	2.7
hPDE5A	>10000	formulatability (mg/mL)[d]	4
hPDE6AB	>10000	CYP450 (>50% inhibition @ 5 μM)[e]	none
hPDE7A	>10000	AMESII[f]	negative
hPDE9A	>10000		
rPDE10A	**480**		
hPDE11A	6920		

[a]Percent metabolized after incubating 1 μM solution 15 min with rLM or hLM at 37 °C. [b]Compound concentration after 4 h incubation in buffer pH 7.4. [c]Determined by potentiometric titration (25 °C). [d]20% HPβCD at pH > 3.5. [e]Enzymatic inhibition of CYP1A2, 2C9, 2D6, 2C19, and 3A4. [f]Adaptation of the colorimetric AMESII Mutagenicity Assay kit from Xenometric. Compound concentration 125 μg/mL.

respectively, with an IC_{50} value of 29 and 480 nM. This is in line with the previously reported values for compound **2**. In addition **6** did not show significant inhibition of a panel of CYP450 enzymes (CYP1A2, 2C9, 2D6, 2C19, and 3A4). The compound was also inactive up to a concentration of 125 μg/mL in a bacterial mutagenicity assay (AMESII). The *in vitro* metabolic stability of **6** was greatly improved both in human (hLM) and rat (rLM) liver microsomes when compared to **2**.

The PK properties of compound **6** were studied in rats after 2.5 mg/kg i.v. and 10 mg/kg p.o. administration (Table 2). After i.v. administration, a rapid clearance was observed ($t_{1/2}$ = 0.47 h), which was not expected based on the *in vitro* metabolic stability in rLM (Table 1). Interestingly, **6** showed much slower clearance after p.o. administration ($t_{1/2}$ = 2.36 h), resulting in good bioavailability and a maximum plasma concentration (C_{max}) of 997 ng/mL.

The good *in vitro* profile and acceptable PK properties of **6** prompted us to explore the possibility of increasing the selectivity of this chemical series versus PDE10. Introducing a lipophilic group to the meta-position of the phenyl on the triazole ring can induce an open Leu770 protein conformation allowing the ligand to access a hydrophobic roof pocket, increasing selectivity versus PDE10.[9] Hence a focused set of analogues **9**−**18** bearing an additional substituent on the 2-chlorophenyl group in **6** was synthesized, and their *in vitro* potency and selectivity were determined (Table 3).

Analogues having a meta-substituted phenyl (**9**−**15**) or pyridyl (**18**) on the pyrido[4,3-*e*][1,2,4]triazolo[4,3-*a*]pyrazine core displayed increased PDE2 selectivity versus PDE10. For instance, introduction of a *n*-butoxy group as in **9** resulted in a

DOI: 10.1021/ml500463t
ACS Med. Chem. Lett. 2015, 6, 282−286

Table 2. Pharmacokinetic Properties of 6 in Rats[a]

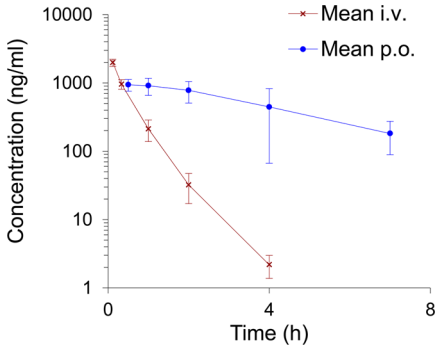

	mean i.v.		s.d.
C_o (ng/mL)	3021	±	388
$t_{1/2}$ (h)	0.47	±	0.08
V_{dz} (L/kg)	1.61	±	0.55
V_{dss} (L/kg)	1.02	±	0.10
Cl (mL/min/kg)	38.7	±	6.5
$AUC_{0\text{-}inf}$ (ng·h/mL)	1042	±	184
	mean p.o.		s.d.
C_{max} (ng/mL)	997	±	241
t_{max} (h)	1.17	±	0.76
$t_{1/2}$ (h)	2.36	±	0.46
$AUC_{0\text{-}inf}$ (ng·h/mL)	4229	±	1892
bioavailability (%)	100		

[a]Male Sprague–Dawley rat fed (n = 3 per time point); i.v., 2.5 mg/kg; p.o., 10 mg/kg.

Table 3. *In Vitro* PDE2 and PDE10 Inhibition and Metabolic Stability Data for Compounds 6 and 9–18

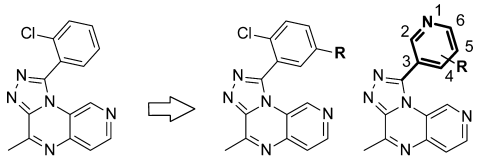

6 9-15 16-18

	R	hPDE2 IC_{50} (nM)[a]	rPDE10 IC_{50} (nM)[a]	rLM[b]	hLM[b]
6	H	29	480	13	7
9	O*n*-Bu	6	5500	98	34
10	$O(CH_2)_2OMe$	95	9120	18	5
11	CH_2O*n*-Pr	21	3890	98	78
12	$CH_2OCH_2CF_3$	3	2450	77	12
13	CH_2O*i*-Pr	10	6030	98	57
14	morpholine	310	>10000	53	14
15	OCF_3	150	8910	11	3
16	5-Cl	5750	n.m.	n.m.	n.m.
17	4-Me	2450	n.m.	n.m.	n.m.
18	5-O*n*-Bu	54	3800	46	6

[a]Average value of at least two independent experiments. [b]Percent metabolized after incubating 1 μM solution 15 min with rLM or hLM at 37 °C.

very potent PDE2 inhibitor with 917-fold selectivity over PDE10. Docking of **9** in the active site of PDE2 (Figure 1) confirmed a similar binding mode as seen in the X-ray structure of **3** (PDB 4D08)[9] and also that of a similar tricyclic molecule binding to PDE10 (PDB 3SNI).[12] The molecule sits in the hydrophobic clamp between Phe862 and Phe830 and forms the typical H-bond interaction with conserved Gln859. As seen in the previously reported series,[9] the triazolo ring forms two water mediated H-bonds to Tyr655 and Gln812. The *n*-butoxy group binds in the lipophilic pocket formed by hydrophobic residues Leu770, Leu809, Ile866, and Ile870. The close proximity of Met847 to the ligand at the site entrance can be seen.

The binding mode of **9** helps to rationalize the observed SAR. The PDE2 activity of 2-methoxyethoxy derivative **10** is 16-fold lower than for **9**, suggesting that polar moieties in the chain are not preferred in the lipophilic roof pocket. The morpholine in **14** is also detrimental for activity likely due to the polarity and suboptimal steric fit. Shifting the ether to the benzylic position as in **11**–**13** is allowed, with **12** being the most potent selective PDE2 inhibitor identified in this exploration (PDE2 IC_{50} = 3 nM, PDE10 IC_{50} = 2450 nM). Interestingly, the trifluoromethyl group in **15** results in a 5-fold decrease in potency (IC_{50} = 150 nM) when compared to **6**, which may be due to an orthogonal orientation of this group. Pyridyls with small substituents, **16** and **17**, were significantly lower in activity. Combination of the *n*-butoxy group in **9** with the distal pyridyl reduced PDE2 activity: molecule **18** was 9-fold less potent than **9**. Of note is that, similar to **6**, analogues **9**–**18** displayed high selectivity over other tested PDEs (see SI).

This exploration and our previous work[9] reveal an interesting SAR originating from the phenyl/pyridyl group, its substitution, orientation, and ability to access the Leu770 lipophilic roof pocket. Induced binding and dynamic effects are not easily studied with conventional docking approaches. Therefore, to investigate these effects more sophisticated modeling based on FEP+ free energy calculations were employed (see SI for details and ΔG^0 values).[13,14] Seven compounds (**6**, **9**, **10**, **12**, **15**, **16**, and **17**) were studied covering a range of activity and substitution patterns while having sufficient similarity to permit reliable structural perturbations between pairs of molecules. The computational results had good agreement with experimental values (R^2 = 0.79, mean unsigned error 0.54 kcal/mol) suggesting the approach captures the molecular details of the ligand enzyme interactions.

Compounds **9** and **12** were correctly predicted to be the most potent inhibitors with approximately equivalent predicted binding free energies. Compounds **16** and **17** were also predicted to be nearly equipotent but with the least favorable binding free energies. These two compounds were more mobile during the simulations, indicating a less tight fit into the binding site. Compounds **10** and **15** were predicted to have nearly equipotent binding free energies and were correctly ranked with intermediate level of potency. Hence, the more hydrophilic linear side chain in the 5-position of **10** as well as the smaller trifluoromethoxy group of **15** produce weaker inhibitors compared to the more lipophilic chain of, e.g., **9**. The binding free energy for **6** deviated most from experiment being underpredicted by ca. 2 kcal/mol. This is understandable as the unsubstituted 2-chlorophenyl binds optimally to a different PDE2 protein conformation compared to that used to start this set of FEP calculations (see SI for further discussion). Molecular dynamics (MD) calculations also shed further light on the conformational flexibility of Leu770 depending on the bound ligand structure. We found that on a simulation time scale of 30 ns, ligands with a large, linear side chain in the phenyl ring 5-position induce a more open form of the lipophilic roof pocket, while for ligands with no 5-substituent

DOI: 10.1021/ml500463t
ACS Med. Chem. Lett. 2015, 6, 282–286

the crucial Leu770 dihedral angle exhibits higher flexibility (see SI for details). Given these promising results we are further studying the FEP+ approach for the design of PDE2 inhibitors.

Unfortunately, the most potent compounds **9**, **12**, and **13** were metabolically unstable when tested *in vitro* against hLM and mainly rLM. An improvement in rat metabolic stability profile was obtained for pyridyl analogue **18**. Prediction of human CYP3A4, 2D6, and 2C9 related metabolism using StarDrop 5[15] and analysis of physicochemical properties as well as structural elements associated with metabolism revealed a nice correlation between predicted compound site liabilities and *in vitro* metabolism with hLM. Especially aliphatic chains pending from the distal phenyl (Table 3, R-group) were predicted to introduce metabolic liabilities, with alkoxymethylene groups correctly being predicted inferior to alkoxy groups (see SI for a comparison between **6**, **9**, **13**, and **18**). The fact that increasing polarity (as in **18**) or fluorination of the side chain (as in **12** and **15**) effectively improves hLM metabolism *in vitro* supports these predictions.

Compounds **6**, **9**−**12**, and **18** were assessed for their potential to cross the blood−brain barrier in rats after 10 mg/kg s.c. administration. All tested compounds showed good formulatability with 10 to 20% HPβCD at pH > 3.5. Brain exposure for **9**−**12** and **18** was lower compared to **6**; nevertheless, the brain concentration for these compounds after 1 h administration was in the range of 370−895 ng/g with high brain free fractions and brain/plasma ratios (Table 4).

Table 4. Total Brain Level Comparison between 6, 9−12, and 18[a,b]

cmpd	6	9	10	11	12	18
f_u, brain (rat)[c]	>0.30	0.026	0.17	0.10	0.10	>0.30
brain 1 h (ng/g)	2730	807	801	895	370	789
B/P 1 h	0.65	0.69	0.44	0.98	1.1	0.61

[a]Male Sprague−Dawley rat fed (n = 2 per time point) 10 mg/kg s.c. [b]Compounds were formulated with 20% HPβCD at pH 3.5−4. [c]Estimated unbound drug fraction to rat brain homogenates after 5 h incubation at 37 °C using a Rapid Equilibrium Dialysis device.

Target engagement of pyrido[4,3-*e*][1,2,4]triazolo[4,3-*a*]-pyrazines **6**, **12**, and **18** was evaluated in an *in vivo* occupancy study in rats using tritiated **3** as radioactive tracer (10 μCi i.v.). In this experiment, MP-10 (2.5 mg/kg s.c.),[16] a potent and selective PDE10 inhibitor was predosed since it was found to greatly increase the signal-to-noise ratio of the tracer. This can be explained by the fact that PDE10 inhibition increases intracellular cGMP, which is known to activate PDE2 through its GAF domain.[17] Using this protocol we could demonstrate that the PDE2/PDE10 inhibitor **6** occupies PDE2 with an ED_{50} of 21 mg/kg (Figure 2) after p.o. administration. For the highly selective PDE2 inhibitor **12** no occupancy was seen up to 10 mg/kg after p.o. dosing, most probably due to poor oral bioavailability. However, when **12** was dosed s.c., high PDE2 occupancy was observed, with an ED_{50} of 3.6 mg/kg. Interestingly compound **18**, despite its good potency and brain exposure, gave a poor occupancy of 23% at the highest tested dose of 10 mg/kg s.c. (see SI).

In summary we have described the design, synthesis, and pharmacological characterization of a novel series of selective and brain penetrant PDE2 inhibitors. Also, we have shown a promising application of free energy perturbation and molecular dynamics calculations to predict the SAR of the

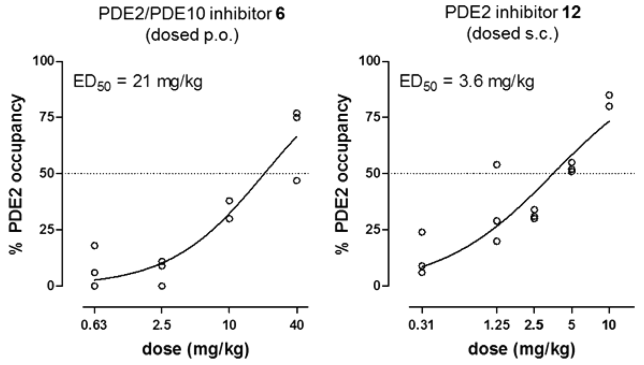

Figure 2. *In vivo* dose/PDE2 occupancy graphs for compounds **6** and **12** (rats, n = 3/dose).

Leu770 lipophilic roof pocket. Two representative compounds from this chemical class have been evaluated *in vivo*. Compared to our previous reports these molecules offer an alternative tricyclic scaffold with improved metabolic stability in some cases permitting target engagement by oral administration. More specifically, compound **6**, which is orally bioavailable, occupied PDE2 with an ED_{50} of 21 mg/kg, a significant improvement over previously reported compound **2**. In addition the highly selective PDE2 inhibitor **12** showed high occupancy after s.c. administration with an ED_{50} of 3.6 mg/kg. These compounds contribute valuable probes to further study the role of PDE2 and PDE10 *in vivo* across a variety of CNS disorders.

■ ASSOCIATED CONTENT

Ⓢ Supporting Information

Computational docking, FEP and Molecular Dynamics calculation protocols, protocols for measuring inhibition of PDEs *in vitro*, selectivity data for **9**−**15** and **18**, *in vivo* occupancy protocols and occupancy data for **18**, CYP3A4 metabolism predictions for **6**, **9**, **13**, and **18**, and the experimental details of the synthesis of key intermediates and compounds **6** and **9**−**18**. This material is available free of charge via the Internet at http://pubs.acs.org.

■ AUTHOR INFORMATION

Corresponding Author

*Phone: +32-14608216. E-mail: frombout@its.jnj.com.

Author Contributions

The manuscript was written through contributions of all authors. All authors have given approval to the final version of the manuscript.

Notes

The authors declare no competing financial interest.

■ ACKNOWLEDGMENTS

We thank Ilse Lenaerts for performing the occupancy experiments. We also thank Geert Pille for measuring the pK_a of **5** and **6**. Finally, we thank Dr. Gerhard Gross for performing and interpreting the StarDrop metabolic site predictions.

■ ABBREVIATIONS

$AUC_{0\text{-inf}}$, area under the curve until infinite time; C_o, zero concentration; B/P, brain-to-plasma ratio; cAMP, cyclic adenosine monophosphate; cGMP, cyclic guanosine monophosphate; Cl, clearance; FEP, free energy perturbation;

DOI: 10.1021/ml500463t
ACS Med. Chem. Lett. 2015, 6, 282−286

HPβCD, (2-hydroxypropyl)-beta-cyclodextrin [128446-35-5]; hLM, human liver microsomes; i.v., intravenous; n.m., not measured; PDE, phosphodiesterase; p.o., *per os* (oral); s.c., subcutaneous; s.d., standard deviation; rLM, rat liver microsomes; $t_{1/2}$, half-life; t_{max}, time at maximum concentration; V_{dss}, steady-state volume of distribution; V_{dz}, apparent volume of distribution

REFERENCES

(1) Francis, S. H.; Blount, M. A.; Corbin, J. D. Mammalian cyclic nucleotide phosphodiesterases: molecular mechanisms and physiological functions. *Physiol. Rev.* **2011**, *91*, 651−90.

(2) Rosman, G. J.; Martins, T. J.; Sonnenburg, W. K.; Beavo, J. A.; Ferguson, K.; Loughney, K. Isolation and characterization of human cDNAs encoding a cGMP-stimulated 3′,5′-cyclic nucleotide phosphodiesterase. *Gene* **1997**, *191*, 89−95.

(3) Lakics, V.; Karran, E. H.; Boess, F. G. Quantitative comparison of phosphodiesterase mRNA distribution in human brain and peripheral tissues. *Neuropharmacology* **2010**, *59*, 367−74.

(4) Gomez, L.; Breitenbucher, J. G. PDE2 inhibition: potential for the treatment of cognitive disorders. *Bioorg. Med. Chem. Lett.* **2013**, *23*, 6522−27.

(5) Schmidt, C. J. Phosphodiesterase inhibitors as potential cognition enhancing agents. *Curr. Top. Med. Chem.* **2010**, *10*, 222−30.

(6) Sanderson, T. M.; Sher, E. The role of phosphodiesterases in hippocampal synaptic plasticity. *Neuropharmacology* **2013**, *74*, 86−95.

(7) Maurice, D. H.; Ke, H.; Ahmad, F.; Wang, Y.; Chung, J.; Manganiello, V. C. Advances in targeting cyclic nucleotide phosphodiesterases. *Nat. Rev. Drug Discovery* **2014**, *13*, 290−314.

(8) Andrés, J.-I.; Buijnsters, P.; De Angelis, M.; Langlois, X.; Rombouts, F.; Trabanco, A. A.; Vanhoof, G. Discovery of a new series of [1,2,4]triazolo[4,3-*a*]quinoxalines as dual phosphodiesterase 2/phosphodiesterase 10 (PDE2/PDE10) inhibitors. *Bioorg. Med. Chem. Lett.* **2013**, *23*, 785−90.

(9) Buijnsters, P.; Andrés, J.-I.; De Angelis, M.; Langlois, X.; Rombouts, F.; Sanderson, W.; Tresadern, G.; Ritchie, A.; Trabanco, A.; Vanhoof, G.; Van Roosbroeck, Y. Structure-based design of a potent, selective, and brain penetrating PDE2 inhibitor with demonstrated target engagement. *ACS Med. Chem. Lett.* **2014**, *5*, 1049−1053.

(10) Friesner, R. A.; Banks, J. L.; Murphy, R. B.; Halgren, T. A.; Klicic, J. J.; Mainz, D. T.; Repasky, M. P.; Knoll, E. H.; Shelley, M.; Perry, J. K.; Shaw, D. E.; Francis, P.; Shenkin, P. S. Glide: A new approach for rapid, accurate docking and scoring. 1. Method and assessment of docking accuracy. *J. Med. Chem.* **2004**, *47*, 1739−1749.

(11) Synthetic protocols are provided as SI. Compounds **6** and **7** have been previously reported in: Joergensen, M.; Bruun, A. T.; Rasmussen, L. K. Preparation of pyridine compounds useful for treating neurological and psychiatric disorders. *PCT Int. Appl.*, WO 2013034761 A1, 2013.

(12) Malamas, M. S.; Ni, Y.; Erdei, J.; Stange, H.; Schindler, R.; Lankau, H.-J.; Grunwald, C.; Fan, K. Y.; Parris, K.; Langen, B.; Egerland, U.; Hage, T.; Marquis, K. L.; Grauer, S.; Brennan, J.; Navarra, R.; Graf, R.; Harrison, B. L.; Robichaud, A.; Kronbach, T.; Pangalos, M. N.; Hoefgen, N.; Brandon, N. J. Highly potent, selective, and orally active phosphodiesterase 10A inhibitors. *J. Med. Chem.* **2011**, *54*, 7621−7638.

(13) Jorgensen, W. L. Efficient drug lead discovery and optimization. *Acc. Chem. Res.* **2009**, *42*, 724−733.

(14) Chodera, J. D.; Mobley, D. L.; Shirts, M. R.; Dixon, R. W.; Branson, K.; Pande, V. S. Alchemical free energy methods for drug discovery: Progress and challenges. *Curr. Opin. Struct. Biol.* **2011**, *21*, 150−160.

(15) *StarDrop* Optibrium, Ltd.: Cambridge, U.K.; http://www.optibrium.com (accessed Dec 19, 2014).

(16) Verhoest, P. R.; Chapin, D. S.; Corman, M.; Fonseca, K.; Harms, J. F.; Hou, X.; Marr, E. S.; Menniti, F. S.; Nelson, F.; O'Connor, R.; Pandit, J.; Proulx-Lafrance, C.; Schmidt, A. W.; Schmidt, C. J.; Suiciak, J. A.; Liras, S. Discovery of a novel class of phosphodiesterase 10A inhibitors and identification of clinical candidate 2-[4-(1-methyl-4-pyridin-4-yl-1*H*-pyrazol-3-yl)-phenoxymethyl]-quinoline (PF-2545920) for the treatment of schizophrenia. *J. Med. Chem.* **2009**, *52*, 5188−96.

(17) Zoraghi, R.; Corbin, J. D.; Francis, S. H. Properties and functions of GAF domains in cyclic nucleotide phosphodiesterases and other proteins. *Mol. Pharmacol.* **2004**, *65*, 267−78.

DOI: 10.1021/ml500463t
ACS Med. Chem. Lett. 2015, 6, 282−286